

Decoding canola and oat crop health and productivity under drought and heat stress using bioelectrical signals and machine learning

Guoqi Wen*, Bao-Luo Ma

Ottawa Research and Development Centre, Agriculture and Agri-Food Canada, 960 Carling Ave., Ottawa, ON K1A 0C6, Canada

ARTICLE INFO

Article history:

Received 17 December 2024

Received in revised form 19 February 2025

Accepted 19 April 2025

Available online xxxx

Keywords:

Abiotic stress

Avena sativa L.

Bioelectrical signal

Brassica napus L.

Random Forest

ABSTRACT

Abiotic stresses, such as heat and drought, often reduce crop yields by harming plant health. Plants have evolved complex signaling networks to mitigate environmental impacts, making monitoring in-situ biosignals a promising tool for assessing plant health in real time. In this study, needle-like sensors were used to measure electrical potential changes in oat and canola plants under heat and drought stress conditions. Signals were recorded over a 30-min period and segmented into time intervals of 1-, 5-, 10-, 20-, and 30-min. Machine learning algorithms, including Random Forest, K-Nearest Neighbors, and Support Vector Machines, were applied to classify stress conditions and estimate biomass based on 14 extracted bioelectrical features, such as signal amplitude and entropy. Results showed that heat stress primarily altered signal patterns, whereas drought stress affected the signal intensity, possibly due to a reduction in the flow rate of charged ions. Random Forest classifier successfully identified over 85 % of stressed crops within 30 min of signal recording. These signals also explained 58–95 % of the variation in plant aboveground and root biomass, depending on stress intensity and crop genotype. This study demonstrates the potential of using bioelectrical sensing as a rapid and efficient tool for stress detection and biomass estimation. Future research should explore the ability to use biosensors to capture genetic variability to mitigate abiotic stresses and combine this with remote sensing and other emerging precision agriculture technologies.

© 2025 © His Majesty the King in Right of Canada, as represented by the Minister of Agriculture and Agri-Food Canada. Publishing services by Elsevier B.V. on behalf of KeAi Communications Co., Ltd. This is an open access article under the CC BY-NC-ND license (<http://creativecommons.org/licenses/by-nc-nd/4.0/>).

1. Introduction

Global climate change is dramatically altering growing conditions for major crops, with extreme weather events such as prolonged droughts and heatwaves becoming more frequent and severe (Zeng et al., 2023). These environmentally induced stressors pose significant challenges to agricultural productivity, leading to substantial yield declines and threatening global food security. A meta-analysis reported that heat and drought stress reduced crop yields by 33 % and 48 %, respectively, while their combined impacts caused an average yield reduction of 65 % (Cohen et al., 2021). Certain flowering crops such as canola (*Brassica napus* L.) are particularly sensitive to high temperature stress, with yield losses exceeding 60 % due to pollen abortion and pollination failure (Wu et al., 2021). In extreme cases, drought events coupled with heat stress can result in up to 85 % of crop yield reductions (Wen et al., 2023a). A four-year study in eastern Canada found that abnormally high temperatures and erratic precipitation caused canola yield losses of 20 % and 9 %, respectively (Wen et al., 2021). Therefore,

it is crucial to develop rapid and effective methods to assess plant health degradation across broad heat and drought gradients. This foundational step is vital for implementing effective and sensitive targeted remediation strategies to mitigate the negative impacts of these environmental stressors.

The adverse effects of weather-related stresses on crop production are primarily attributed to their impacts on the physiological, chemical, and morphological functions. For example, high temperatures can severely disrupt plant photosynthesis and respiration by impairing enzyme activity, chloroplast function, and the electron transport chain (Allakhverdiev et al., 2008; Posch et al., 2019). Water shortages, on the other hand, significantly hamper water and nutrient uptake, leading to nutritional imbalances that alter root growth, reduce leaf expansion, and impair plant metabolism (Gonzalez-Dugo et al., 2010; Roupael et al., 2012). Both stressors also trigger the accumulation of reactive oxygen species (ROS) in plant tissues, damaging cellular functions and inhibiting plant growth (Tripathy and Oelmüller, 2012). These changes are regulated through intricate signaling networks within plants (Gong et al., 2010; Gui et al., 2021), affecting the transmission of electrical signals among cells, tissues, and organs through modifications in membrane potential, ion channels, and transporters (Zhang et al., 2023;

* Corresponding author.

E-mail address: guoqi.wen@agr.gc.ca (G. Wen).

<https://doi.org/10.1016/j.aiaa.2025.04.006>

2589-7217/© 2025 © His Majesty the King in Right of Canada, as represented by the Minister of Agriculture and Agri-Food Canada. Publishing services by Elsevier B.V. on behalf of KeAi Communications Co., Ltd. This is an open access article under the CC BY-NC-ND license (<http://creativecommons.org/licenses/by-nc-nd/4.0/>).

Zhu, 2016). This represents the electrical potential difference between two points within the plant, enabling rapid response to external changes and long-distance information transmission (Napier et al., 2022; Zhang et al., 2023). Therefore, accurately measuring this potential in real time provides a potential approach for assessing plant health under abiotic stress conditions.

The shoot and root systems are where plants grow and develop, interact with the environment, and receive stimulation from biotic and abiotic stressors. Leaves on plant shoots drive energy conversion efficiency through photosynthesis and sugar transport and fundamentally determine yield formation, while roots anchor the plant, absorb water and nutrients, and send hormone signals to aid stress adaptation (Kalra et al., 2024; Li et al., 2021), ultimately affecting productivity. Therefore, precise measurement of aboveground shoot biomass and belowground root biomass can provide rapid and reliable indicators to quantify crop responses to environment-induced stresses. To date, various methods have been developed and validated for quantifying root and shoot biomass, including traditional approaches such as excavating and measuring roots (Wen and Ma, 2024) and manually collecting aboveground shoots to determine their mass in the laboratory. Several rapid and innovative non-destructive methods have also been reported. For example, electrical capacitance and impedance measurements have been widely tested for estimating root traits under stress (Cseresnyés et al., 2021; Wu et al., 2017), based on the principle that plant root tips act as ion storage cylinders, forming a resistance-capacitance circuit at the soil-root interface (Dalton, 1995; Augé and Stodola, 1990; Goraya et al., 2017). However, their reliability is influenced by soil conditions, as dry soil reduces conductivity, and overly wet soil can cause current leakage, leading to inconsistent readings (Gu et al., 2021). Satellite-acquired imagery provides a powerful tool for estimating crop biomass under diverse growing conditions (Dong et al., 2016). However, its effectiveness is often limited by the complex geometry of plant shoots and their variable environmental exposure (Fang et al., 2021). The scale of canopy size monitored hinders its use in fine-tuning plant phenotyping in variety improvement programs. Therefore, significant gaps remain in the development of precise, scalable, and real-time monitoring tools to assess plant responses to environmental stresses. Furthermore, methods capable of simultaneously quantifying root and shoot traits are still lacking.

In this study, we adapted a compact, needle-shaped electrical sensor to measure bioelectrical signals in canola and oat (*Avena sativa* L.) plants subjected to heat and drought stress. The sensor captured voltage differences between two points in plant tissues, reflecting electrochemical activities driven by metabolic processes and ion transport. Machine learning algorithms were developed based on bioelectrical signals to classify plant stress conditions and estimate biomass. Additionally, we explored the underlying mechanisms of stress-induced changes in bioelectrical signaling. We hypothesized that healthy plants would display stable and robust electrical signals, indicative of normal metabolic and physiological processes, while stressed plants would exhibit altered electrical patterns, reflecting disruptions in ion transport and cellular function. By integrating bioelectrical signals with machine learning-based predictive models, this study can improve our understanding of plant responses to environmental stress and develop early stress monitoring systems and new methods for biomass estimation, thus filling gaps in plant phenotyping analysis.

2. Materials and methods

2.1. Experimental design

We conducted three experiments on canola and oat crops in growth chambers and greenhouses in 2021–2022 to evaluate the viability and

performance of a newly introduced signal sensor across different growing environments.

Exp I: Canola heat experiment. The study was conducted in a split-plot design under chamber-controlled environments. Air temperature variation across different growth chambers was the main plot factor, and canola hybrid (InVigor L233P and InVigor L252) within each chamber was the subplot factor. Three hybrid seeds were sown in each biodegradable pot (15 cm in diameter × 15 cm in height) and were thinned to one plant per pot at 7 days after planting (DAP). After planting, pots were transferred to growth chambers (Model GR 96, CONVIRON, Controlled Environment Ltd., Winnipeg, MB) to facilitate seed germination. The heat treatment commenced at 20 DAP for 10 days, adhering to a 24-h cycle designed to simulate the typical meteorological temperature variations observed during the canola growing season in Ottawa, ON, Canada (Biswas et al., 2019). The heat treatment was patterned as: 2:01–10:00 = 23 °C, 10:01–11:00 = 26 °C, 11:01–12:00 = 29 °C, 12:01–16:00 = 32 °C, 16:01–17:00 = 29 °C, 17:01–18:00 = 26 °C, 18:01–22:00 = 23 °C, 22:01–2:00 = 26 °C, while the control chamber was maintained at a constant 23/17 °C (light/dark).

Exp II: Canola drought experiment. This greenhouse study was carried out in a split-plot design, where watering level was assigned as the main plot factor and canola hybrid as subplot. The hybrids used were InVigor L233P, noted for its drought tolerance, and InVigor L252, known for its sensitivity to drought based on a prior field study (Wen et al., 2023b). Three seeds were initially sown in each pot (16.5 cm in diameter × 16.5 cm in height) and thinned to one seedling at 10 DAP. Plants were subjected to three watering levels – well-watered as control, moderate drought, and severe drought during two critical growth stages: vegetative (4 true leaves) and early flowering (20 % flowering). The watering treatment lasted for 15 days and an automated irrigation system equipped with capacitive soil moisture sensors (Capacitive Soil Moisture Sensor v1.2) and Raspberry Pi as controllers. Soil moisture levels were maintained at 80–85 % water holding capacity (WHC) for control conditions, 55–65 % WHC for moderate drought, and 35–45 % WHC for severe drought, which were calibrated using soil moisture set SM150T with HH2 meter. After treatment, the watering was adjusted to maintain WHC at 80–85 % until the crop matured. In this study, we merged signals measured at both growth stages, focusing specifically on using these signals as indicators of different watering levels.

Exp III: Oat drought experiment. The experimental design and management details are elaborated in Wen et al. (2023a). Briefly, the experiment consisted of 30 oat varieties grown in cone pots. A total of 8 oat seeds were sowed and thinned to four plants per pot at 10 DAP. At the heading stage, the watering regime was adjusted to maintain soil moisture at 80–85 % WHC in the control group, and 35–45 % WHC in the drought treatment group for 15 days. Prior to and following the treatment phases, all pots were well watered to ensure at least 80 % WHC.

For all three experiments, the soil mix used to fill the pots consisted of sieved topsoil, vermiculite, peat moss, and perlite in a 6:1:1:1 volume ratio, with its physiochemical properties reported in Wu et al. (2017). All treatments were fertilized with an N-P₂O₅-K₂O ratio of 20–20–20 and applied bi-weekly (0.1 g per container for oat and 1 g per pot for canola). Both the growth chambers and greenhouses were set to a consistent 16/8-h light/dark cycle. In the drought experiments, the air temperature was maintained at 25 °C during the day and 18 °C at night, with 45–55 % relative humidity and a minimum photosynthetic photon flux density (PPFD) of 300 $\mu\text{mol m}^{-2} \text{s}^{-1}$ on cloudy days. For the canola heat experiment, the chambers provided a PPFD of approximately 500 $\mu\text{mol m}^{-2} \text{s}^{-1}$ at canopy level and maintained 70–75 % relative humidity. The environment in the growth chambers was continuously monitored at 5-min intervals using a BOHO logger, while the environmental conditions in the greenhouses were regulated using an ARGUS platform. The canola heat experiment was replicated seven times, and the drought experiments were replicated four times.

2.2. Sample collection

Plant electrical signals were recorded using a needle-like biosensor, which consisted of coaxial cable (2.8 mm diameter) with central conductor wire (silver coated copper filament diameter < 0.5 mm) incorporated into the PhytSigns platform (Vivent Sàrl, Crans-près-Celigny, Switzerland). This platform, powered by a Raspberry Pi 4B with an alternating current (AC) to direct current (DC) converter, digitized the sensed data to ensure accurate measurements. To stabilize signal acquisition, for canola, the positive electrode was inserted deeply into the conductive bundle of the first fully developed green leaf from the bottom; and for oat, it was inserted into the stem 5–7 cm above the soil surface (Fig. 1, 2a, 3c, and 4b). The negative electrode was positioned at the root crown about 1–2 cm above the soil surface. Our experiments were carefully designed to ensure that needle insertion, maintenance, and monitoring were in the same locations and exerted similar forces on treated and control plants. To minimize the impact of water during plant watering, the contact points between the plant tissue surface and the signal sensor were sealed with melted wax. Electrodes were checked every 10-min, twice per session, to ensure stability and replace as needed. Data were recorded as electric potential over time and stored as raw files on the Raspberry Pi. The electrical frequency during sampling was set to 256 Hz, meaning that 256 signal voltage data points were collected per second. In this study, biosignal monitoring was performed carefully and uniformly on treated and control plants by the same personnel, taking into account the week intensity of electrical signals and the potential damage caused by bioneedle insertion. Additionally, a control study was conducted in which a subset of plants was left uninserted to compare their growth and physiological responses with

sensor-equipped plants. No significant differences were observed in biomass accumulation or stress responses between the two groups, suggesting that the insertion strategy did not introduce measurable interference with plant physiology or electrical signal measurements. To ensure consistency, stable signal data recorded approximately 3-h after needle insertion were selected for comparative analysis between heat- or drought-stressed plants and their respective controls.

In Exp I, the entire canola plants were harvested immediately after the treatment ended by cutting them just above the soil surface. The above-ground parts were sectioned into 1–2 cm pieces and stored in envelopes. The roots were thoroughly cleaned and then scanned. Both the roots and shoots were dried at 80 °C for one week to determine dry biomass. In Exp II and III, the plants were collected after reaching maturity and then divided into shoots and roots, following the same protocol as Exp I. This included sectioning, cleaning, scanning, and drying to measure dry biomass. Across all three experiments, our goal was to evaluate whether signal measurements can be utilized for early biomass estimation. Predesigned signal data durations were selected for comparison between treated and control plants to eliminate interference with circadian rhythms.

2.3. Data processing

Once the plant signals were recorded, the raw data were extracted and converted into parquet format using Python (Version 3.11.5). Subsequently, the signal series were loaded into a DataFrame and segmented into intervals of 1, 5, 10, 20, and 30 min. Since light intensity, O₂/CO₂ concentration, humidity, and temperature in growth chambers and greenhouses were automatically adjusted, the motor-forced air

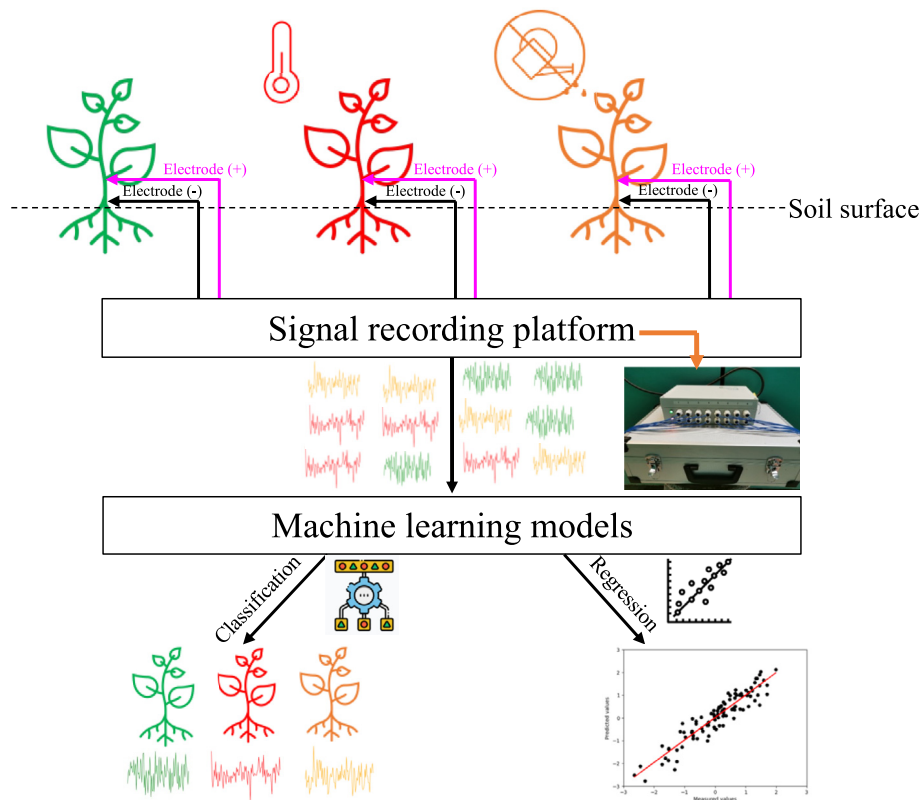


Fig. 1. The overview scheme of electrical signal measurement and data analysis in studies of heat and drought stress in canola and oat plants. Electrode placement: For canola, the positive electrode was inserted into the petiole of the first fully developed green leaf starting from the bottom, and for oat plants, it was inserted into the first extended internode starting from the bottom. Negative electrodes were positioned in the root crown, about 0.5 cm above the soil surface. Signal recording and processing: Signals were recorded at a frequency of 256 samples sec^{-1} and segmented into intervals of 1, 5, 10, 20, and 30 min for detailed feature extraction and analysis. Machine learning prediction: Use different models to classify plant health status and predict plant below- and above-ground biomass. (For interpretation of the references to colour in this figure legend, the reader is referred to the web version of this article.)

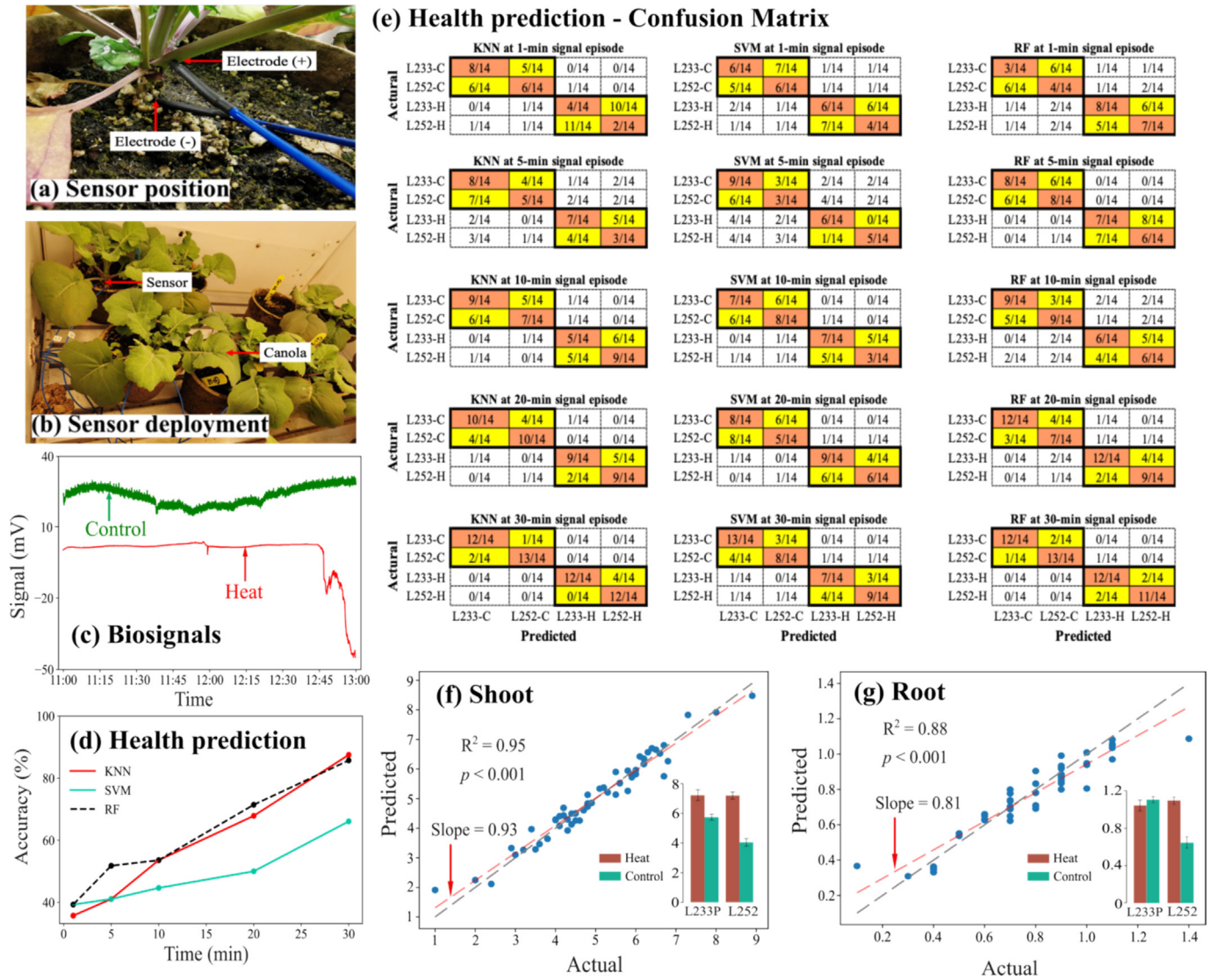


Fig. 2. Canola response to heat stress and predictive modeling performance. (a) Placement of electrodes in canola for signal capture in the petiole and root crown zone. (b) Biosensor and canola plants deployment in the chamber. (c) Signal recorded over a 2-h period in control and heat-treated plants, showing lower values in heat-stressed canola. (d) Accuracy in predicting the effect of heat stress using machine learning models: K-Nearest Neighbors (KNN), Support Vector Machines (SVM), and Random Forest (RF). (e) Confusion matrix illustrating the performance of machine learning algorithms in identifying heat stress tolerance levels of different canola varieties. (f) & (g) RF-based predictions for shoot and root biomass from 30-min signal episodes, with embedded bar plots displaying biomass under heat and control conditions for different hybrids. R^2 values, p -values, and regression slopes demonstrate the correlation between predicted and actual values, with the ideal 1:1 line indicating perfect predictions.

gas exchange was expected to cause signal irregular fluctuations in the signal. The watering and fertilization process could also cause additional disturbances. Therefore, we adopted windowing with a step size of 100 and first-order differencing techniques to remove noisy signals because of their high effectiveness (Priyanka, 2017). Following noise removal, several preprocessing steps were undertaken to refine the data, which included feature extraction, normalization, and labeling. For each signal episode, we extracted 14 distinct features (Table 1) and normalized these features using the formula:

$$X = \frac{x - \bar{x}}{\sigma}$$

where X , x , \bar{x} , σ represent the normalized feature vector, the noise-removed signal data, the arithmetic mean, and the standard deviation of the signal data, respectively.

2.4. Establishment of machine learning algorithms

To assess plant health, we utilized three supervised machine learning classifiers: K-Nearest Neighbors (KNN), Random Forest (RF), and Support Vector Machines (SVM) based on the sklearn package in Python (version 3.11). The hyperparameters for each algorithm were optimized through 10-fold cross-validation to enhance model reliability and performance. Due to the limited size of the dataset, model performance was primarily evaluated using the leave-one-out cross-validation procedure. Since the RF classifier performed superior to other models, particularly in the oat experiment and the demonstrated power of RF in forecasting grain yield and optimal N rates (Wen et al., 2021; Wen et al., 2022), its regressor was further applied to predict shoot and root biomass. Simple regression analysis was conducted between the actual and predicted values. The coefficient of determination

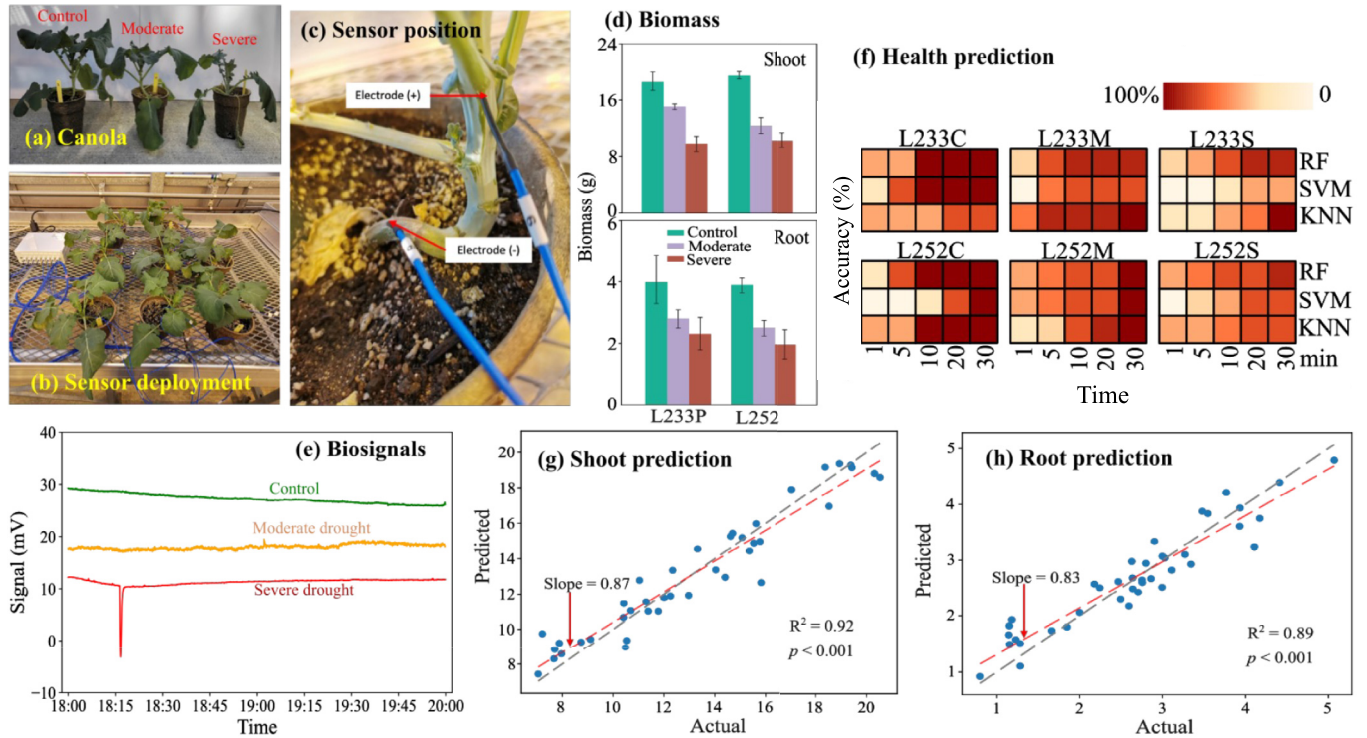


Fig. 3. Canola response to drought stress and predictive modeling outcomes. (a) Canola health status under various irrigation treatments. (b) Overview of biosensor deployment. (c) Insertion points of biosensor electrodes in the canola plants. (d) Effects of drought on shoot and root biomass in specific canola hybrids. (e) Signal variation over 2 h for control, moderate, and severe drought-stressed canola. (f) Prediction accuracy for drought stress effects using K-Nearest Neighbors (KNN), Support Vector Machines (SVM), and Random Forest (RF). (g) & (h) Predictions of shoot and root biomass using RF based on 30-min signal episodes, with R^2 values and p -values indicating model accuracy and statistical significance. Regression line slopes and the 1:1 line demonstrate the correlation between predicted and actual values. L233C, L233M, and L233S represent the control, moderate, and severe drought of canola hybrid L233. Similarly, L252C, L252M, and L252S refer to the control, moderate, and severe drought of canola hybrid L252.

(R^2), p -value, and the slope of the regression equation were used to evaluate the model's prediction performance. Once acceptable results for plant health detection and biomass estimation were determined, the features of the 30-min signal measurements were further analyzed using relative importance analysis with RF to examine how heat or drought stress affected signal patterns. Furthermore, Pearson correlation analysis was performed to determine the relationship between these signal features and crop shoot and root biomass.

3. Results

3.1. Biosignaling responses to abiotic stress

Analysis of raw electrical signals showed that healthy canola exhibited a more stable signal potential with an average of 26 mV during the 30-min measurements. Heat exposure significantly reduced signal strength by up to 57 % (Fig. 2c). Interestingly, the signal changes were not always synchronized with changes in air temperature but showed significant delays depending on the measurement time point and air temperature. For example, an increase in air temperature from 26 to 29 °C resulted in a visual signal drop after one hour, while a further increase in temperature to 32 °C led to a rapid signal drop within 45-min (Fig. 2c). Interestingly, this reduction in signal intensity is the opposite direction of the signal and absolute value of the electrical potential may have actually increased. Drought stress also significantly affected the signal potential, with signal intensity decreased by up to 59 % in stressed plants (Fig. 3e). As soil moisture decreased, plant signal potential dropped systematically from 27 mV under control conditions to 11 mV under severe drought. Compared to canola, oat crops exhibited larger signal fluctuations over time, as shown in both healthy and drought-affected plants (Fig. 4c). Healthy oat plants displayed signal

voltages ranging from 12 to 16 mV, while plants under drought conditions showed a gradual decrease in signal potential from 6 to 2 mV over the course of 30 min of measurement.

Analysis of the signal feature importance across different growing environments revealed that SET was the most influential factor during the heat-stress experiment, followed by basic statistical metrics (Fig. 5a). On the contrary, signal SUM emerged as the most critical feature under drought treatment (Fig. 5b and c). Considering the definition of each feature in Table 1, we concluded that heat stress primarily increased the complexity of electrical potential change pattern, making the signals more irregular. In contrast, drought stress had minimal impacts on signaling patterns, as indicated by the lower importance of STM.

3.2. Biosignals-based plant health detection

Using machine learning models to identify stressed crops, signal measurement efficiently and rapidly distinguished plant health status. Within the 1-min signal measurements, KNN identified over 89 % (25 out of 28) of healthy and 96 % (27 out of 28) of heat-stressed canola plants (Fig. 2e). Although SVM and RF performed less effectively, they still detected over 80 % of stressed plants. With continuous signal recording, the plant health identification capacity progressively increased to over 90 % for all three models with 30-min signal measurements. Interestingly, we observed significant improvements in overall prediction accuracy over time, suggesting that longer signal windows provided more detailed insights into canola hybrid-specific plant health. For instance, within the first minute, the models correctly detected 36–39 % of canola hybrid and treatment combinations, and after 30 min of signal measurement, the accuracy of the KNN and RF models increased to 86 % (Fig. 2d). SVM performance lagged, identifying

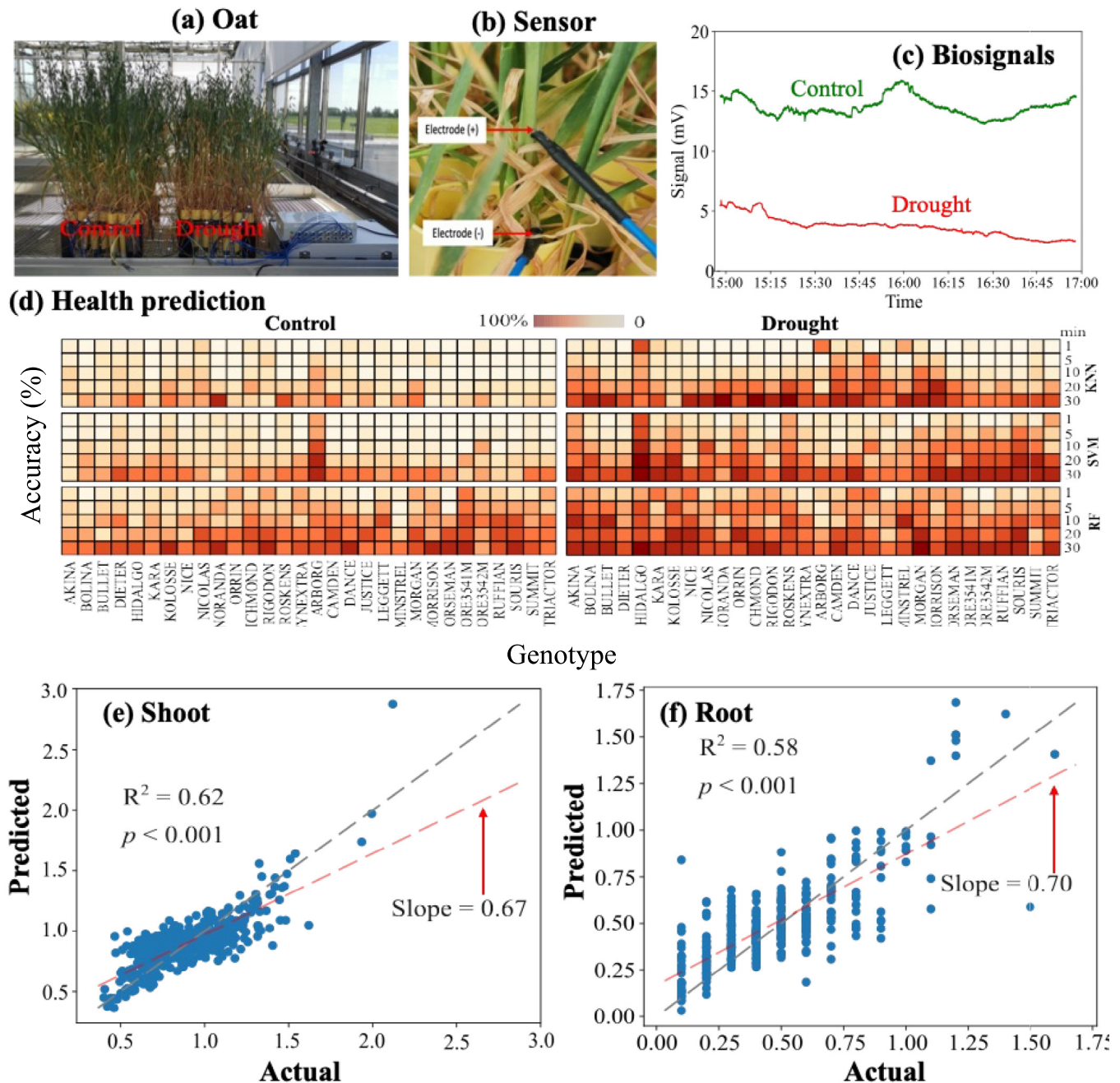


Fig. 4. Oat response to drought stress and predictive modeling outcomes. (a) Oat growth under control and drought conditions. (b) Illustration of electrode attached position in plants for signal capture. (c) Raw signals from control and drought-treated oats recorded over two hours. (d) Prediction accuracy of machine learning models of K-Nearest Neighbors (KNN), Support Vector Machines (SVM), and Random Forest (RF) using different time-based signal episodes. (e) & (f) RF predictions of oat shoot and root biomass based on 30-min signal episodes, with R^2 values and p -values indicating the model's predictive power and statistical significance, respectively. The regression line slopes and the 1:1 line show the relationship between predicted and actual values.

approximately 66 % of hybrid-treatment combinations after 30 min of signal measurement. Likewise, in drought studies, extending the signal measurement time progressively captured the environmental factors of soil moisture and the distinct responses of individual cultivars (Fig. 3f). In the study of 30 oat cultivars responding to drought, 30-min signal measurements successfully identified more than 70 % of cultivar \times drought groups (Fig. 4d). Overall, the signal measurement easily distinguished healthy and stressed plants, but its ability to explore the variability between crop cultivars posed a challenge to the accuracy of short-term signals. Across three experiments, the RF model consistently outperformed the other two machine learning models in detecting

plant health status. Therefore, below we used the RF algorithm in the next step to estimate plant shoot and root biomass.

3.3. Shoot and root biomass estimation

In Exp I, shoot biomass of healthy canola plants averaged 4.7 g plant⁻¹ for Invigor L233P and 3.3 g plant⁻¹ for Invigor L252. The high temperature treatment significantly increased shoot biomass by 26 % for Invigor L233P and 78 % for Invigor L252 (Fig. 2f). Meanwhile, heat stress increased the root biomass of InVigor 252 by an average of 70 %, whereas the root biomass of InVigor L233P did not change (Fig. 2g).

Table 1

Features used for establishing models, along with their explanations and calculation formulas.

Features	Functions/Explanations	Formulas
Mean	Arithmetic mean of the data points.	$Mean = E[x_i]$
Minimum (Min)	The smallest value in a dataset.	
Maximum (Max)	The largest value in a dataset.	
Median	The middle value in a dataset, calculated by arranging the data in ascending order and then finding the middle value.	When n is odd: $Median = x_{\frac{n+1}{2}}$ When n is even: $Median = \frac{1}{2}(x_{\frac{n}{2}} + x_{\frac{n}{2}+1})$
Lower quartile (Q1)	Q1 separates the lower 25 % of data from the higher 75 %, calculated by arranging the data in ascending order and then finding the 1/4th value.	$Q1 = \frac{n+1}{4}^{th} \text{ Term}$ where Term presents the signal series with the attribute that the data values are from smallest to largest.
Upper quartile (Q3)	Q3 separates the lower 75 % of data from the higher 25 %, calculated by arranging the data in ascending order and then finding the 3/4th value.	$Q3 = \frac{3 \times (n+1)}{4}^{th} \text{ Term}$ where Term presents the signal series with the attribute that the data values are from smallest to largest.
Summation (Sum)	The sum value of data points.	$SUM = \sum_{i=1}^n x_i$
Variance (Var)	Var reflects the distance of each data point from the mean value in the dataset, measuring the degree of dispersion between data points.	$Var = E[x_i - \mu]^2$
Standard deviation (Std)	Square root of variance.	$Std = \sqrt{Var}$
Kurtosis (KURT)	KURT measures the probability distribution of a random variable and describes the shape of the probability distribution.	$KURT = E\left[\frac{x_i - \mu}{\sigma}\right]^4$
Skewness (SKEW)	SKEW describes the asymmetry of a dataset with a normal distribution. The sign of SKW indicates which side the data are skewed (positive value = right, negative value = left).	$SKEW = E\left[\frac{x_i - \mu}{\sigma}\right]^3$
Log energy entropy (LEE)	LEE provides the complexity and regularity of the signals.	$LEE = -\sum_{i=1}^n P_i \times \log(P_i)$ where P_i is the normalized log-energy value for each segment.
Sample entropy (SE)	SE measures the complexity of time-series signals. Greater SE values indicate higher complexity, while smaller values characterize more self-similar and regular signals.	$SE = -\log \frac{C(3, 0.2\sigma)}{C(2, 0.2\sigma)}$ where $C(3, 0.2\sigma)$ is the number of embedded vectors of length 3 having a Chebyshev distance inferior to 0.2σ and $C(2, 0.2\sigma)$ is the number of embedded vectors of length 2 having a Chebyshev distance inferior to 0.2σ .
Sample entropy (SET)	SET quantifies the regularity or predictability of signal datasets. Lower values indicate more self-similarity (regularity) in the data while higher values indicate more randomness/complexity in the datasets.	$SET(m, r, N) = -\ln\left(\frac{B}{A}\right)$ where m is the embedding dimension (segment length), r is the similarity tolerance, N is the time series length, A is the count of sequence pairs of length m + 1 within r, and B is the count of sequence pairs of length mm within r.

These features were derived through modifications of those described in [Tran et al. \(2019\)](#).

Both canola hybrid cultivars exhibited a similar decrease in shoot and root biomass of approximately 50 % when subjected to drought stress (Fig. 3d). Similar effects of drought stress were observed for oat biomass, as detailed in [Wen et al. \(2023a\)](#).

After 30 min of recording, signal measurements explained 95 % of the shoot biomass in the canola heat stress experiment, predicting an actual biomass slope of 0.93 (Fig. 2f). This indicated that for lower biomass the predicted values were slightly higher and vice versa for higher biomass above 5.5 g plant⁻¹. A similar pattern was observed in the canola drought stress study, where 30-min signals accounted for about 92 % of shoot biomass (Fig. 3g). However, in the oat experiment consisting of 30 cultivars, the predictive accuracy dropped significantly, with an R² of 0.62 and a slope of 0.67, showing discrepancies in biomass estimation, especially for plant biomass above 1.4 g plant⁻¹ (Fig. 4e). In contrast, root biomass predictions were less accurate. The 30-min signal explained 88 % of the actual root biomass in the experiment involving two canola cultivars and different temperatures (Fig. 2g). The same signal episode explained 89 % of root biomass across three drought conditions for the canola cultivars (Fig. 3h). The biosignal sensor profiled a significant decline in predicting root biomass across 30 oat cultivars, with an R² of 0.58 and slope of 0.70, highlighting the challenge of accurately predicting root biomass in tests involving multiple diverse genotypes (Fig. 4f).

Analyzing the linear relationships between biomass and signal features revealed that root and aboveground plant biomass were primarily related to SET in the canola heat stress experiment (Fig. 6). In the canola drought experiment, biomass increased or decreased linearly with most signal features. This linear relationship was less evident in the oat drought experiment, suggesting that the predictive accuracy of the linear model may decrease as classification complexity increases.

4. Discussion

4.1. Effects of stress on plant biomass

The frequency of extreme heat events during summer is increasing, significantly impacting the productivity of main field crops. In this study we observed that heat stress during the vegetative stage significantly increased both shoot and root biomass in canola (Fig. 2f and g). This is completely different to those subjected from heat stress during the flowering stage, where high air temperatures damaged fertility organs, disrupted physiological enzyme activities, and affected pollination, ultimately reducing the overall productivity of canola crops ([Wen et al., 2021](#); [Wu et al., 2020](#)). For example, our recent field studies conducted across Canada revealed that yield responses to nutrient supply in over 80 % of the cases were significantly affected by drought, heat, or a combination of both ([Wen et al., 2023b, 2024](#)). [Biswas et al. \(2019\)](#) and [Wollenweber et al. \(2003\)](#) reported that the physiological response of plants to heat stress depends on temperature and growth stage and a moderate increase in temperature during the early growth stages may actually enhance the rate of photosynthesis and dry matter accumulation. Thus, the vegetative stage may have a higher temperature threshold value because the maximum temperature was higher than the threshold value of 29.5 °C for flowering canola reported by [Morrison and Stewart \(2002\)](#). Additionally, higher air temperatures accelerated plant evapotranspiration rates ([Biswas et al., 2019](#)), and sufficient watering helped cool leaf temperatures, ensuring continued enzyme activity and nutrient uptake by roots, which resulted in higher biomass accumulation. In contrast, drought stress reduced both shoot and root biomass of canola and oat crops primarily due to decreased nutrient uptake and utilization, reduced leaf area, and lower photosynthetic rates ([Wu et al., 2018](#); [Zhao et al., 2021](#)).

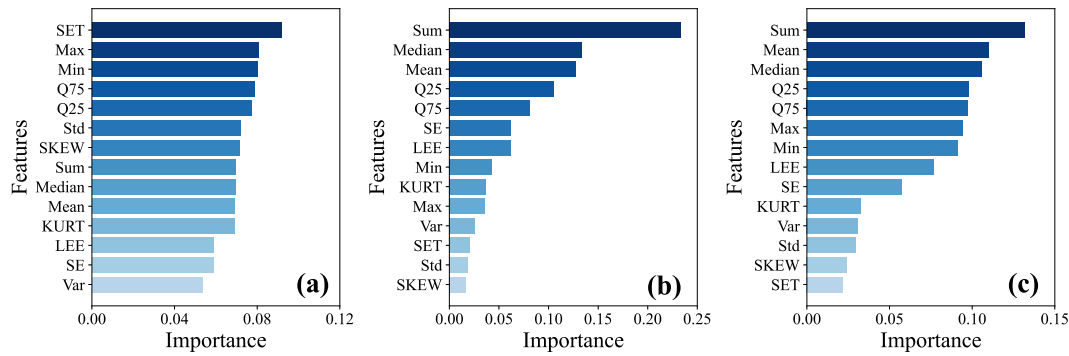


Fig. 5. The relative importance for each feature extracted from signal measurements during 30-min episodes for treatment prediction in Exp I (a), Exp II (b), and Exp III (c) using random forest methods. In Exp I, predictions were made for four combinations of two genotypes and two temperature treatments. In Exp II, classifications involved two genotypes and three drought levels. In Exp III, predictions encompassed thirty genotypes and two drought levels.

4.2. Effects of stress on biosignals

In all three experiments, we observed fluctuating signals in both healthy and stressed plants. These signal variations were determined by complex internal biochemical and physiological metabolic activities within the plant tissues, as well as charged ionic flow through the plant's vascular system caused by the surrounding environment (Tran et al., 2019). For canola plants under controlled conditions, the relatively stable electrical potential indicated preserved ion homeostasis, membrane integrity, and nutrient element uptake, which are essential for healthy plant growth and development. However, complex patterns of signal variations were observed when subjected to heat treatment (Fig. 2c and Fig. 5a). This is largely due to the complex temperature settings, designed to simulate the full 24-h diurnal temperature cycle observed in Ottawa during the summer. Using a threshold value of 29.5 °C for canola (Morrison and Stewart, 2002), the plants only experienced heat stress between 12:00 and 16:00. Thus, elevated temperatures before the stress period (e.g., 11:00–12:00) initially stimulated enzyme activity and metabolic processes, enhancing water and nutrient absorption and the activity of ion pathways. However, during the stress

period, prolonged exposure to high temperatures disrupted membrane stability and ion fluxes, leading to rapid accumulation of ROS and the transient transmission of electrical signals in plants for hormone regulation (Elferjani and Soolanayakanahally, 2018; Grinberg et al., 2022). These physiological and biochemical changes alter the function of ion channels and pumps, leading to shifts in ion concentrations, particularly the loss of K^+ and the influx of Ca^{2+} , which may lead to electrical signals to propagate rapidly, triggering downstream protection mechanisms, such as stomatal closure, antioxidant enzyme activation, and stress-related gene expression (Demidchik, 2010; Tripathy and Oelmüller, 2012; Bhattacharya, 2019; Lamaoui et al., 2018). These electrical changes are consistent with known pathways in abiotic stress signaling, including the abscisic acid and jasmonic acid response networks. Additionally, to reduce leaf temperatures under heat stress, plants need to increase water uptake from the soil, prioritizing water over nutrient absorption. Higher water influx may cause dilution of the charged ion concentration in the xylem sap, resulting in a decrease in electrical voltage values (Fig. 2c).

Our data showed that drought stress reduced the electrical potential between the stem and root crown in both canola and oat plants, which

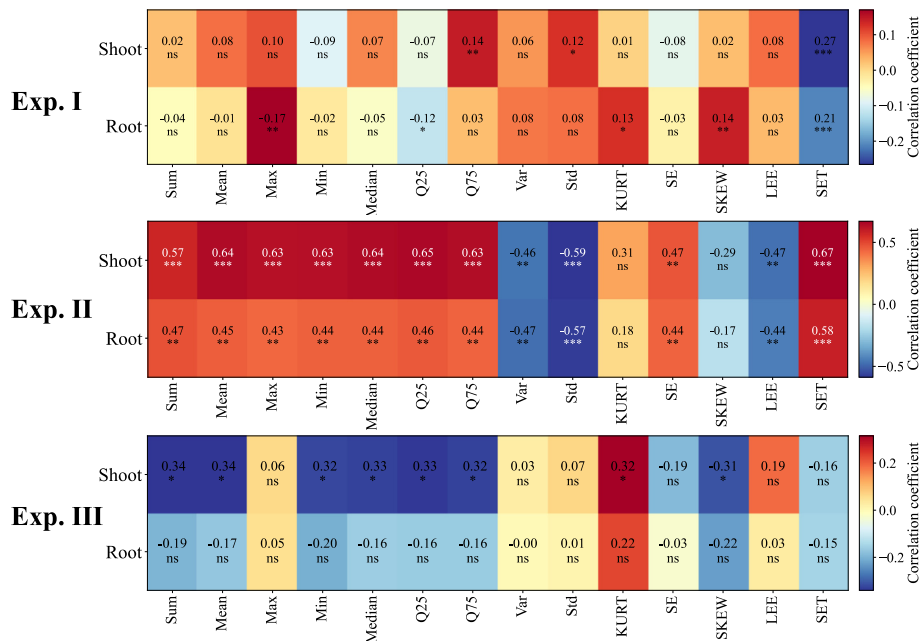


Fig. 6. The simple correlation coefficients for each feature extracted from signal measurements during 30-min episodes with the shoot and root biomass for Exp I, II, and III. The ns, or *, **, and *** indicate not significant at $p < 0.05$, or significant at $0.01 \leq p < 0.05$, $0.001 \leq p < 0.01$, and $p < 0.001$, respectively.

was mainly attributed to the reduced water potential and photosynthetic electron transport (Pukacki and Kamińska-Rożek, 2005). As soil moisture reduction-induced soil nutrients unavailability for root uptake and cavitation of plant xylem hinder the transport of mineral elements in the xylem and decrease the voltage difference between the stem and root crown (Choat et al., 2015; Seleiman et al., 2021). At the cellular level, water scarcity in plants can dramatically disrupt the delicate ion gradients across cellular membranes, which in turn hindered the signal communication (Gil et al., 2008) and reduced electrical potential between the roots and leaves (Fig. 3e and 4e). However, as drought stress persists and intensifies, the plant adaptive responses gradually weaken, and prolonged drought reduced the effectiveness of these mechanisms (Lata et al., 2015; Yang et al., 2021). This is in good agreement with our findings, which showed that drought stress primarily affected the electrical potential values (e.g., Sum, Mean, and Median metrics) and has a relatively small impact on signal pattern complexity (Fig. 5b and c).

4.3. Plant health indication and biomass estimation

In this study, we explored the feasibility of using signal measurement with machine learning algorithms to identify plant responses to the duration and extent of heat and drought stress. Among the three models tested, RF demonstrated the highest predictive accuracy. This may be attributed to its ensemble learning approach, which reduces overfitting, effectively handles nonlinear relationships, and manages missing data better than KNN and SVM. The performance of KNN was likely limited by its sensitivity to noisy data, while SVM may have struggled with parameter optimization and computational complexity. Across all three models, the progressive improvement in prediction accuracy over monitoring time vividly underscores the importance of capturing extended physiological data for robust stress detection in plants (Fig. 2e, 3f, and 4d). Within short observation windows, it was efficiently to detect stressed plants from healthy ones. However, distinguishing crop cultivars with same health status, such as different oat cultivars under drought conditions, was challenging. This was mainly because similar signal patterns were observed between plants of the same treatment, whereas the signal changed significantly when crops were stressed compared to health plants. As signals were continuously measured, the underlying detailed patterns between cultivars were progressively identified. For example, when we extended the signal period from 1 min to 30 min, the accuracy of the RF model improved significantly from 39 % to 85 % (Fig. 2d), which was mainly due to the improved accuracy in identifying the cultivars.

The observed differences in shoot and root biomass responses to external heat and drought stress, coupled with the high accuracy of signal-based crop health predictions, suggest that signal measurements may be an effective method to quantify plant biomass. This is because plant biomass is the result of photosynthesis and the assimilation of nutrients absorbed from the soil and air through biochemical processes involved in the transmission of signaling networks (Irving, 2015; Shiade et al., 2024). This conclusion is well supported by our results that signal estimates accounted for 67 % to 95 % of variation in belowground and aboveground biomass, outperforming some high-throughput phenotyping methods such as estimates based on drone imagery (Wang et al., 2021). This suggests that the introduction of bio-electrical signals could be a major advance in the convergence of biotechnology and digital technologies, allowing plant scientists and agronomists to predict and address potential agricultural challenges early or to select targeted plant genotypes in breeding programs. However, additional features and further model refinement are needed to enhance health status and biomass predictions across various crop varieties and genotypes. Continuous advancements in machine learning models, supported by a deeper understanding of plant abiotic stress physiology, are crucial for developing reliable and broadly applicable predictive tools in agriculture.

4.4. Optimizing bioelectrical sensing for agricultural applications

Conventional methods of assessing plant stress and biomass, such as visual observation and destructive sampling, are labor-intensive and time-consuming. While high-throughput alternatives like thermal imaging and spectral reflectance indices offer efficiency, they require specialized equipment. In contrast, bioelectrical sensing provides a low-cost, real-time, and continuous monitoring solution with the potential for high accuracy and scalability, particularly in controlled environments such as breeding programs rapid generation advancement in plant and crop greenhouse production. However, scaling up monitoring for field applications based on bioelectrical signals faces challenges due to environmental factors like soil heterogeneity, wind, plant-to-plant variations among plant populations. Additionally, power supply and data transmission for continuous monitoring pose logistical challenges, necessitating energy-efficient and wireless sensor networks. Despite these obstacles, advances in sensor miniaturization, machine learning-driven signal processing, and Internet of Things (IoT) technologies could support real-time, large-scale deployment of precision agriculture, enabling early stress detection and improved biomass estimation.

This study demonstrated the ability of bioelectrical sensing to enable early detection of physiological responses to heat and drought stress through electrical potential monitoring, which correlates well with biomass measurements. However, the complexity of signal processing and the mildly invasive nature of needle insertion remain concerns. Future research should focus on optimizing sensor placement, improving data interpretation, and integrating bioelectrical sensing with remote sensing technologies to enhance precision and field applicability. In addition, a cost-benefit analysis is necessary to compare bioelectrical sensing with conventional stress detection and biomass estimation methods to evaluate its practical advantages and challenges.

5. Conclusions

In this study, we documented that biosignals measured by needle-shaped sensors displayed distinct patterns between healthy and stressed plants. Machine learning algorithms effectively captured these patterns to quantify plant health status within 30-min of monitoring, with performance influenced by the complexity of the experiment, particularly the number of genotype-by-treatment combinations. In this study, we found that heat stress primarily disrupted signal patterns, increasing their irregularity and unpredictability. In contrast, drought stress affected signal intensity, likely reflecting a reduced flow rate of charged ions through the plant stems. The microsensors used, combined with advanced machine learning models, could be valuable tools for agronomists and plant researchers aiming to rapidly select superior crop cultivars with better tolerance to unpredictable environmental stresses.

While this study highlights the potential of using bioelectrical signals for biomass estimation, the accuracy varied due to factors like electrode placement, plant development, and environmental fluctuations. Refining signal processing and integrating complementary sensing, such as hyperspectral imaging, could improve reliability. Further research should focus on bioelectrical sensing through deep learning, multi-sensor fusion, and large-scale field trials. Wireless and IoT-enabled sensor networks will enhance real-time monitoring and accelerate the adoption of sustainable crop management.

CRediT authorship contribution statement

Guoqi Wen: Writing – review & editing, Writing – original draft, Visualization, Project administration, Methodology, Investigation, Formal analysis, Data curation, Conceptualization. **Bao-Luo Ma:** Funding acquisition, Supervision, Writing – review & editing.

Declaration of competing interest

The authors declare no competing interests.

Acknowledgements

This study was financially supported by the Agriculture and Agri-Food Canada (AAFC) Canadian Agricultural Partnership (CAP) and Sustainable Canadian Agricultural Partnership (SCAP) programs with the Eastern Canada Oilseed Development Alliance (ECODA), Canadian Field Crop Research Alliance (CFCRA), and Canadian Institute of Food Science and Technology (CIFST) through collaborative research and development agreements between AAFC and ECODA, between AAFC and CFCRA, and between AAFC and CIFST, Project J-000249, Project J-000292, Project J-002164, and Project J-003376. We thank Dr. Weikai Yan, oat breeder at the AAFC Ottawa Research and Development Centre (ORDC), for providing the oat genotypes used in this study. Thanks also to Lynne Evenson, Alex Quesnel, and Olivia Rideout for sample collection, and to Rachel Gendron and Daniel Casselman for growth chamber and greenhouse maintenance. AAFC-ORDC contribution no. 25-005.

Data availability

We have no additional data associated with the manuscript to be deposited.

References

- Allakhverdiev, S.I., Kreslavski, V.D., Klimov, V.V., Los, D.A., Carpentier, R., Mohanty, P., 2008. Heat stress: an overview of molecular responses in photosynthesis. *Photosynth. Res.* 98, 541–550. <https://doi.org/10.1007/s11200-008-9331-0>.
- Augé, R.M., Stodola, A.J.W., 1990. An apparent increase in symplastic water contributes to greater turgor in mycorrhizal roots of droughted *Rosa* plants. *New Phytol.* 115, 285–295. <https://doi.org/10.1111/j.1469-8137.1990.tb00454.x>.
- Bhattacharya, A., 2019. Chapter 1 - effect of high-temperature stress on crop productivity. In: Bhattacharya, A. (Ed.), *Effect of High Temperature on Crop Productivity and Metabolism of Macro Molecules*. Academic Press, pp. 1–114. <https://doi.org/10.1016/B978-0-12-817562-0.00001-X>.
- Biswas, D.K., Ma, B.L., Morrison, M.J., 2019. Changes in leaf nitrogen and phosphorus content, photosynthesis, respiration, growth, and resource use efficiency of a rapeseed cultivar as affected by drought and high temperatures. *Can. J. Plant Sci.* 99, 488–498. <https://doi.org/10.1139/cjps-2018-0023>.
- Choat, B., Brodersen, C.R., McElrone, A.J., 2015. Synchrotron X-ray microtomography of xylem embolism in *Sequoia sempervirens* saplings during cycles of drought and recovery. *New Phytol.* 205, 1095–1105. <https://doi.org/10.1111/nph.13110>.
- Cohen, I., Zandalinas, S.I., Huck, C., Fritsch, F.B., Mittler, R., 2021. Meta-analysis of drought and heat stress combination impact on crop yield and yield components. *Physiol. Plant.* 171, 66–76. <https://doi.org/10.1111/ppl.13203>.
- Cseresnyés, I., Mikó, P., Kelemen, B., Füzy, A., Parádi, I., Takács, T., 2021. Prediction of wheat grain yield by measuring root electrical capacitance at anthesis. *Int. Agrophys.* 35, 159–165. <https://doi.org/10.31545/itagr/136711>.
- Dalton, F.N., 1995. In-situ root extent measurements by electrical capacitance methods. *Plant Soil* 173, 157–165. <https://doi.org/10.1007/BF00155527>.
- Demidchik, V., 2010. Reactive oxygen species, oxidative stress and plant ion channels. In: Demidchik, V., Maathuis, F. (Eds.), *Ion Channels and Plant Stress Responses*. Signaling and Communication in Plants. Springer, Berlin, Heidelberg. https://doi.org/10.1007/978-3-642-10494-7_11.
- Dong, T., Liu, J., Qian, B., Zhao, T., Jing, Q., Geng, X., Wang, J., Huffman, T., Shang, J., 2016. Estimating winter wheat biomass by assimilating leaf area index derived from fusion of Landsat-8 and MODIS data. *Int. J. Appl. Earth Obs. Geoinf.* 49, 63–74. <https://doi.org/10.1016/j.jag.2016.02.001>.
- Elferjani, R., Soolanayakanahally, R., 2018. Canola responses to drought, heat, and combined stress: shared and specific effects on carbon assimilation, seed yield, and oil composition. *Front. Plant Sci.* 9, 01224. <https://doi.org/10.3389/fpls.2018.01224>.
- Fang, P., Yan, N., Wei, P., Zhao, Y., Zhang, X., 2021. Aboveground biomass mapping of crops supported by improved CASA model and sentinel-2 multispectral imagery. *Remote Sens.* 13, 2755. <https://doi.org/10.3390/rs13142755>.
- Gil, P.M., Gurovich, L., Schaffer, B., 2008. The electrical response of fruit trees to soil water availability and diurnal light-dark cycles. *Plant Signal. Behav.* 3, 1026–1029. <https://doi.org/10.4161/psb.6786>.
- Gong, D.S., Xiong, Y.C., Ma, B.L., Wang, T.M., Ge, J.P., Qin, X.L., Li, P.F., Kong, H.Y., Li, Z.Z., Li, F.M., 2010. Early activation of plasma membrane H⁺-ATPase and its relation to drought adaptation in two contrasting oat (*Avena sativa* L.) genotypes. *Environ. Exp. Bot.* 69, 1–8. <https://doi.org/10.1016/j.envexpbot.2010.02.011>.
- Gonzalez-Dugo, V., Durand, J.L., Gastal, F., 2010. Water deficit and nitrogen nutrition of crops. A review. *Agron. Sustain. Dev.* 30, 529–544. <https://doi.org/10.1051/agro/2009059>.
- Goraya, G.K., Kaur, B., Asthir, B., Bala, S., Kaur, G., Farooq, F., 2017. Rapid injuries of high temperature in plants. *J. Plant Biol.* 60, 298–305. <https://doi.org/10.1007/s12374-016-0365-0>.
- Grinberg, M., Gromova, E., Grishina, A., Berezina, E., Ladeynova, M., Simakin, A.V., Sukhov, V., Gudkov, S.V., Vodenev, V., 2022. Effect of photoconversion coatings for greenhouses on electrical signal-induced resistance to heat stress of tomato plants. *Plants* 11, 229. <https://doi.org/10.3390/plants11020229>.
- Gu, H., Liu, L., Butnor, J.R., Sun, H., Zhang, X., Li, C., Liu, X., 2021. Electrical capacitance estimates crop root traits best under dry conditions—a case study in cotton (*Gossypium hirsutum* L.). *Plant Soil* 467, 549–567. <https://doi.org/10.1007/s11104-021-05094-6>.
- Gui, Y.W., Sheteiwy, M.S., Zhu, S.G., Batool, A., Xiong, Y.C., 2021. Differentiate effects of non-hydraulic and hydraulic root signaling on yield and water use efficiency in diploid and tetraploid wheat under drought stress. *Environ. Exp. Bot.* 181, 104287. <https://doi.org/10.1016/j.envexpbot.2020.104287>.
- Irving, L.J., 2015. Carbon assimilation, biomass partitioning and productivity in grasses. *Agriculture* 5, 1116–1134. <https://doi.org/10.3390/agriculture5041116>.
- Kalra, A., Goel, S., Elias, A.A., 2024. Understanding role of roots in plant response to drought: way forward to climate-resilient crops. *Plant Genome* 17, e20395. <https://doi.org/10.1002/tpg2.20395>.
- Lamaoui, M., Jemo, M., Datla, R., Bekkaoui, F., 2018. Heat and drought stresses in crops and approaches for their mitigation. *Front. Chem.* 6, 26. <https://doi.org/10.3389/fchem.2018.00026>.
- Lata, C., Muthamilarasan, M., Prasad, M., 2015. Drought stress responses and signal transduction in plants. In: Pandey, G.K. (Ed.), *Elucidation of abiotic stress SIGNALING in Plants, functional Genomics Perspectives*. 2, pp. 195–225. https://doi.org/10.1007/978-1-4939-2540-7_7.
- Li, H., Testerink, C., Zhang, Y., 2021. How roots and shoots communicate through stressful times. *Trends Plant Sci.* 26, 940–952. <https://doi.org/10.1016/j.tplants.2021.03.005>.
- Morrison, M.J., Stewart, D.W., 2002. Heat stress during flowering in summer Brassica. *Crop Sci.* 42, 797–803. <https://doi.org/10.2135/cropsci2002.7970>.
- Napier, J.D., Heckman, R.W., Juenger, T.E., 2022. Gene-by-environment interactions in plants: molecular mechanisms, environmental drivers, and adaptive plasticity. *Plant Cell* 35, 109–124. <https://doi.org/10.1093/plcell/koac322>.
- Posch, B.C., Kariyawasam, B.C., Bramley, H., Coast, O., Richards, R.A., Reynolds, M.P., Trethowan, R., Atkin, O.K., 2019. Exploring high temperature responses of photosynthesis and respiration to improve heat tolerance in wheat. *J. Exp. Bot.* 70, 5051–5069. <https://doi.org/10.1093/jxb/erz257>.
- Priyanka, Kaur G., 2017. Noise removal in ECG signal using windowing technique and its optimization. *Adv. Biotechnol. Microbiol.* 6, 555676. <https://doi.org/10.19080/AIBM.2017.06.555676>.
- Pukacki, P.M., Kamińska-Rożek, E., 2005. Effect of drought stress on chlorophyll a fluorescence and electrical admittance of shoots in Norway spruce seedlings. *Trees* 19, 539–544. <https://doi.org/10.1007/s00468-005-0412-9>.
- Rouphael, Y., Cardarelli, M., Schwarz, D., Franken, P., Colla, G., 2012. Effects of drought on nutrient uptake and assimilation in vegetable crops. In: Aroca, R. (Ed.), *Plant Responses to Drought Stress: From Morphological to Molecular Features*. Springer, Berlin, Heidelberg, pp. 171–195. https://doi.org/10.1007/978-3-642-32653-0_7.
- Seleiman, M.F., Al-Suhaibani, N., Ali, N., Akmal, M., Alotaibi, M., Refay, Y., Dindaroglu, T., Abdul-Wajid, H.H., Battaglia, M.L., 2021. Drought stress impacts on plants and different approaches to alleviate its adverse effects. *Plants* 10, 259. <https://doi.org/10.3390/plants10020259>.
- Shiade, S.R.G., Zand-Silakhoor, A., Fathi, A., Rahimi, R., Minkina, T., Rajput, V.D., Zulfikar, U., Chaudhary, T., 2024. Plant metabolites and signaling pathways in response to biotic and abiotic stresses: exploring bio stimulant applications. *Plant Stress* 12, 100454. <https://doi.org/10.1016/j.stress.2024.100454>.
- Tran, D., Dutoit, F., Najdenovska, E., Wallbridge, N., Plummer, C., Mazza, M., Raileanu, L.E., Camps, C., 2019. Electrophysiological assessment of plant status outside a faraday cage using supervised machine learning. *Sci. Rep.* 9, 17073. <https://doi.org/10.1038/s41598-019-53675-4>.
- Tripathy, B.C., Oelmüller, R., 2012. Reactive oxygen species generation and signaling in plants. *Plant Signal. Behav.* 7, 1621–1633. <https://doi.org/10.4161/psb.22455>.
- Wang, T., Liu, Y., Wang, M., Fan, Q., Tian, H., Qiao, X., Li, Y., 2021. Applications of UAS in crop biomass monitoring: a review. *Front. Plant Sci.* 12, 616689. <https://doi.org/10.3389/fpls.2021.616689>.
- Wen, G., Ma, B.L., 2024. Optimizing crop nitrogen use efficiency: integrating root performance and machine learning into nutrient management. *Adv. Agron.* 187, 311–363. <https://doi.org/10.1016/bs.agron.2024.05.006>.
- Wen, G., Ma, B.L., Vanasse, A., Caldwell, C.D., Earl, H.J., Smith, D.L., 2021. Machine learning-based canola yield prediction for site-specific nitrogen recommendations. *Nutr. Cycl. Agroecosyst.* 121, 241–256. <https://doi.org/10.1007/s10705-021-10170-5>.
- Wen, G., Ma, B.L., Vanasse, A., Caldwell, C.D., Smith, D.L., 2022. Optimizing machine learning-based site-specific nitrogen application recommendations for canola production. *Field Crop Res.* 288, 108707. <https://doi.org/10.1016/j.fcr.2022.108707>.
- Wen, G., Ma, B.L., Shi, Y., Liu, K., Chen, W., 2023a. Selection of oat (*Avena sativa* L.) drought-tolerant genotypes based on multiple yield-associated traits. *J. Sci. Food Agric.* 103, 4380–4391. <https://doi.org/10.1002/jsfa.12504>.
- Wen, G., Ma, B.L., St Luce, M., Liu, K., Mooleki, P.S., Crittenden, S., Gulden, R., Semach, G., Tiege, P., Lokuruge, P., 2023b. Optimizing nitrogen fertilization for hybrid canola (*Brassica napus* L.) production across Canada. *Field Crop Res.* 302, 109048. <https://doi.org/10.1016/j.fcr.2023.109048>.
- Wen, G., Liu, K., Kubota, H., Peng, G., Semach, G., Lokuruge, P., Chau, H.W., Khakbazan, M., 2024. Precipitation and nitrogen management are key drivers of cropping system

- productivity in the Canadian prairies. *Can. J. Plant Sci.* 00, 1–12. <https://doi.org/10.1139/cjps-2024-0114>.
- Wollenweber, B., Porter, J.R., Schellberg, J., 2003. Lack of interaction between extreme high-temperature events at vegetative and reproductive growth stages in wheat. *J. Agron. Crop Sci.* 189, 142–150. <https://doi.org/10.1046/j.1439-037x.2003.00025.x>.
- Wu, W., Duncan, R.W., Ma, B.L., 2017. Quantification of canola root morphological traits under heat and drought stresses with electrical measurements. *Plant Soil* 415, 229–244. <https://doi.org/10.1007/s11104-016-3155-z>.
- Wu, W., Ma, B.L., Whalen, J.K., 2018. Chapter three - enhancing rapeseed tolerance to heat and drought stresses in a changing climate: perspectives for stress adaptation from root system architecture. *Adv. Agron.* 151, 87–157. <https://doi.org/10.1016/bs.agron.2018.05.002>.
- Wu, W., Shah, F., Duncan, R.W., Ma, B.L., 2020. Grain yield, root growth habit and lodging of eight oilseed rape genotypes in response to a short period of heat stress during flowering. *Agric. For. Meteorol.* 287, 107954. <https://doi.org/10.1016/j.agrformet.2020.107954>.
- Wu, W., Duncan, R.W., Ma, B.L., 2021. Crop lodging, pod fertility and yield formation in canola under varying degrees of short-term heat stress during flowering. *J. Agron. Crop Sci.* 207, 690–704. <https://doi.org/10.1111/jac.12510>.
- Yang, X., Lu, M., Wang, Y., Wang, Y., Liu, Z., Chen, S., 2021. Response mechanism of plants to drought stress. *Horticulturae* 7, 50. <https://doi.org/10.3390/horticulturae7030050>.
- Zeng, Z., Wu, W., Peñuelas, J., Li, Y., Jiao, W., Li, Z., Ren, X., Wang, K., Ge, Q., 2023. Increased risk of flash droughts with raised concurrent hot and dry extremes under global warming. *Npj Clim. Atmos. Sci.* 6, 1–12. <https://doi.org/10.1038/s41612-023-00468-2>.
- Zhang, Y., Xu, J., Li, R., Ge, Y., Li, Y., Li, R., 2023. Plants' response to abiotic stress: mechanisms and strategies. *Int. J. Mol. Sci.* 24, 10915. <https://doi.org/10.3390/ijms241310915>.
- Zhao, B., Ma, B.L., Hu, Y., Liu, J., 2021. Source-sink adjustment: a mechanistic understanding of the timing and severity of drought stress on photosynthesis and grain yields of two contrasting oat (*Avena sativa* L.) genotypes. *J. Plant Growth Regul.* 40, 263–276. <https://doi.org/10.1007/s00344-020-10093-5>.
- Zhu, J.K., 2016. Abiotic stress signaling and responses in plants. *Cell* 167, 313–324. <https://doi.org/10.1016/j.cell.2016.08.029>.